



PERGAMON

Available online at www.sciencedirect.com

SCIENCE @ DIRECT®

Electrochimica Acta 48 (2003) 2143–2148

ELECTROCHIMICA
Acta

www.elsevier.com/locate/electacta

Characterization of PVdF-HFP polymer membranes prepared by phase inversion techniques I. Morphology and charge–discharge studies

A. Manuel Stephan¹, Dale Teeters*

Department of Chemistry and Biochemistry, The University of Tulsa, 600 S. College Ave., Tulsa, OK 74104-3189, USA

Received 19 May 2002; accepted 18 December 2002

Abstract

A novel nanoporous polymer membrane comprised of poly(vinylidene fluoride-co-hexafluoropropylene) (PVdF-HFP) copolymer was prepared by phase inversion techniques using two different non-solvents. The films were subjected to scanning electron microscope (SEM) and nitrogen adsorption/desorption analysis. The morphology and porosity of the membranes are correlated with the chemical structure of the non-solvents used. Also, nanoparticle $\text{LiCr}_{0.01}\text{Mn}_{1.99}\text{O}_4$ cathode material was prepared by solid-state reaction followed by ball milling. The prepared samples were analyzed using X-ray diffraction (XRD) and atomic force microscopy (AFM). The charge–discharge behavior of lithium cells made from the coupling of the nanoporous polymer membrane with the $\text{LiCr}_{0.01}\text{Mn}_{1.99}\text{O}_4$ nanoparticle cathode was studied. The cathode nanoparticles resulting from ball milling were found to be more important in enhanced cell performance than the nanostructure of the nanoporous polymer membranes.

© 2003 Elsevier Science Ltd. All rights reserved.

Keywords: Phase inversion; Nanoparticles; Morphology; Nanopores; Solid-state reaction; Charge–discharge studies

1. Introduction

Polymer electrolytes in conjunction with improved cathode materials are receiving considerable attention as components in advanced secondary lithium batteries because of their advantages including safety, high energy density, high single cell voltage, geometry and no memory effect [1,2].

Various processes have been used to improve the polymer electrolyte part of the equation. Gel polymer electrolytes are usually prepared by dissolving polymer, lithium salt and low molecular weight organic plasticizers in a low boiling point solvent [3–5]. The resulting slurry is cast as films. This process, however, requires a

moisture-free environment because of the hydroscopic nature of the lithium salt. Water in polymer electrolytes prepared through this method cause the electrolytes to lose much of their mechanical strength. The mechanical properties of the film can be enhanced either by chemical or mechanical curing, which is expensive. The Bellcore technology [6] attempts to circumvent these problems by using a liquid activation and extraction process to prepare the polymeric electrolyte material for plastic lithium ion batteries. In this process, dibutyl phthalate was used as an additive; however, the conductivity of the film was expectedly low. Enhancement of conductivity was achieved by the addition of fumed silica [7]. Unfortunately, the charging rate of lithium ion cells with these films was poor. The ionic conductivity of porous membranes used in these electrolyte systems mainly depends on the conductivity of the electrolyte entrapped in the pores of the membrane. Therefore, the membrane porosity, conductivity of the electrolyte, thickness of the membrane and the extent to

* Corresponding author. Tel.: +1-918-631-3147; fax: +1-918-631-3404.

E-mail address: dale-teeters@utulsa.edu (D. Teeters).

¹ Present address: Advanced Batteries Division, Central Electrochemical research Institute, Karaikudi 630006, India.

which the electrolyte wets the pores of the membrane are the properties to be considered for the membrane preparation [8–12]. A greater porosity and perhaps smaller pore diameters are two pre-requisites of good separators for rechargeable lithium batteries. Nanoscale engineering, which can address many of the issues mentioned above, holds promise in the development of polymer electrolyte membranes with enhanced properties.

Improvements in the cathodes coupled with polymer electrolyte membranes have also been addressed. For instance, LiMn_2O_4 cathode materials are more compatible with polymer electrolytes than LiCoO_2 and are favored as cathode materials due to low price and low toxicity of manganese. However, the discharge capacity of LiMn_2O_4 cells decreases rapidly upon repeated cycling due to the Jahn–Teller distortion in the manganese oxide spinel structure. This leads to a large fading of the capacity. It has been suggested that the fade in capacity in the 3 V region is due to this distortion and that the reduction in capacity in the 4 V region is due to both the dissolution of spinel into the electrolyte and decomposition of the electrolyte [13]. It has been shown that the substitution of a small amount of a dopant ion in place of Mn ions can improve the cyclability of LiMn_2O_4 .

Nanoscale engineering has also helped the performance of cathode systems. Manev et al. [14] have shown that smaller particles are more flexible than larger particles during cycling and that the changes in the lattice parameters are only slightly affected. Recently, the preparation of nano crystalline cathode materials by ball milling was demonstrated by Li et al. [15], Goodenough et al. [16] and by Stephan and Teeters [17,18]. The benefits of these nano crystalline cathode materials was also shown in these studies [15–18].

The aim of the present work is to study the properties of a lithium battery system composed of a polymer electrolyte membrane and a cathode that have both been engineered on the nanoscale. The charge–discharge behavior of a nanoscale modified $\text{LiCr}_{0.01}\text{Mn}_{1.99}\text{O}_4$ composite cathode material coupled with a nanoporous polymer membrane that was prepared by the relatively new phase inversion technique has been investigated. To the best of our knowledge, little work has been done on the development of PVdF-HFP polymer membranes using different solvents causing different membrane nanoscale morphologies. Ball milling was used to make nanoscale particles of a solid-state-synthesized spinel with composition of $\text{LiCr}_{0.01}\text{Mn}_{1.99}\text{O}_4$. How does the pore morphology of the polymer membranes vary with the solvents used for preparation? Will the nanoscale cathode material be compatible with these highly nanoporous membranes for battery applications? These are some of the questions we have tried to answer.

2. Experimental

2.1. Polymer membrane

Microporous polymer films were obtained by phase inversion technique as described elsewhere [14–19]. PVdF-HFP co-polymer (Elf Atochem, Japan) was dissolved in a mixture of acetone (a volatile solvent) and pentane or 1-butanol (a non-solvent for the polymer). The resulting solutions were cast as films on glass substrates and the solvents were allowed to evaporate at ambient temperature. The initial concentration of the non-solvent was kept low enough to allow solubilization of the polymer. However, as the concentration of the acetone was lowered by evaporation, phase separation of the polymer from the solution occurred. Traces, if any, of the non-solvents were removed by vacuum drying for 12 h at 100 °C. All experiments were performed in a dry room. Morphological examination of the films was made by a JSM-5410LV scanning microscope under a vacuum (10^{-1} Pa) after sputtering gold on one side of the films. The BET surface area and pore-size distribution were determined by a continuous-flow nitrogen gas adsorption/desorption apparatus (BELSORP 28, Japan).

2.2. Preparation of cathode

The $\text{LiCr}_{0.01}\text{Mn}_{1.99}\text{O}_4$ spinel compound was prepared from the stoichiometric mixture of $\text{LiOH}\cdot\text{H}_2\text{O}$, $(\text{NH}_4)_2\text{Cr}_2\text{O}_7$ and $(\text{CH}_3\text{CO}_2)_2\text{Mn}\cdot 4\text{H}_2\text{O}$. The finely ground mixture was burned at 250 °C for 20 h and then calcined at 800 °C for 24 h with intermediate grinding. The prepared compounds were ball milled for 2 h and were characterized by XRD (SCINTAC ID3000, USA) and AFM (Picoscan, Molecular Imaging, USA) analysis.

2.3. Cell

The composite cathode was prepared by brush-coating a slurry of 85% of $\text{LiCr}_{0.01}\text{Mn}_{1.99}\text{O}_4$, 5% of poly(vinylidene difluoride) and 10% acetylene black in 1-methyl-2-pyrrolidinone on an aluminum substrate and drying in a vacuum oven at 120 °C for 12 h. The prepared polymer membranes were soaked in the electrolyte solution of LiPF_6 in an organic solvent composed of ethylene carbonate and dimethyl carbonate having a volume ratio of 2:1. Lithium foil was used as the anode. The $\text{LiCr}_{0.01}\text{Mn}_{1.99}\text{O}_4$ /polymer membrane electrolyte/Li cell was assembled in an argon filled glove box.

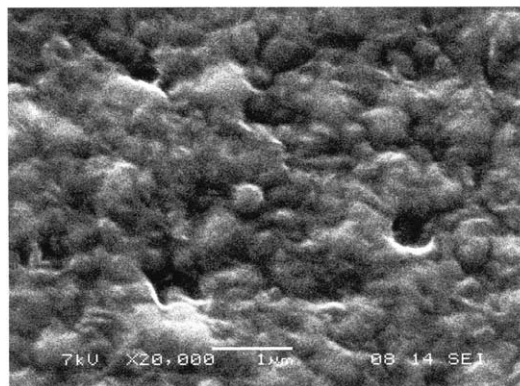
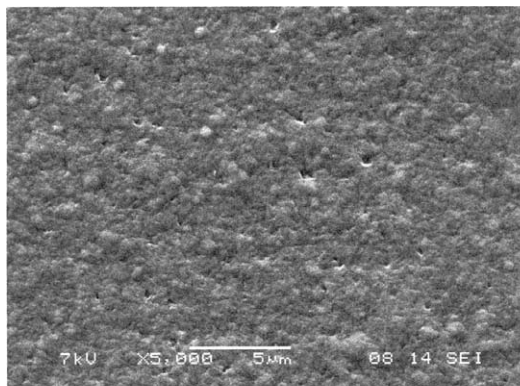


Fig. 1. SEM images of PVdF-HFP membranes prepared with pentane as non-solvent.

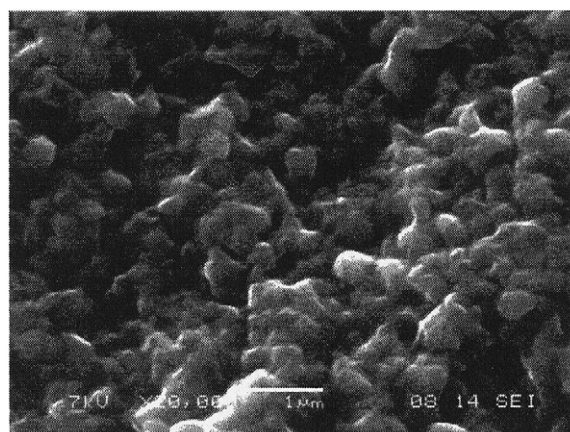
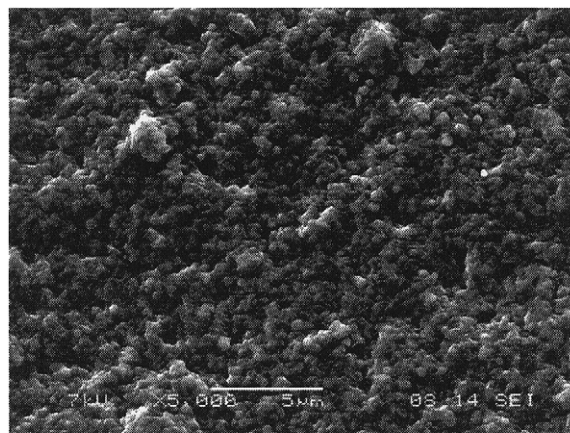


Fig. 2. SEM images of PVdF-HFP membranes prepared with 1-butanol as non-solvent.

3. Results and discussion

SEM images (Figs. 1 and 2) reveal the morphology of the polymer membranes prepared with pentane (Fig. 1) and 1-butanol (Fig. 2) as non-solvents. A homogenous phase with uniformly sized pores was achieved when the linear aliphatic non-solvent, pentane, was used. This compares to a flaky surface with unevenly sized pores developed when 1-butanol as the non-solvent was used. Fig. 3 shows the pore size distribution for the films prepared with pentane and 1-butanol as non-solvents. As shown in Fig. 3, almost all pores of the PVdF-HFP membranes prepared with pentane and 1-butanol are, according to IUPAC conversion, “mesophase”, i.e. pores with diameters ranging from 2 to 50 nm. Celgard 2400, a commonly used polymer membrane separator in lithium batteries, makes for an interesting comparison to the polymer films made here. It is known that Celgard 2400 separators possess a mean pore diameter of 26 nm and a BET surface area of $41.76 \text{ m}^2 \text{ g}^{-1}$ [19]. The films prepared in this work with pentane and 1-butanol as non-solvents exhibit pore diameters and BET surface areas of 12 nm and $120 \text{ m}^2 \text{ g}^{-1}$ and 40 nm and $48 \text{ m}^2 \text{ g}^{-1}$, respectively. The PVdF-HFP membrane prepared

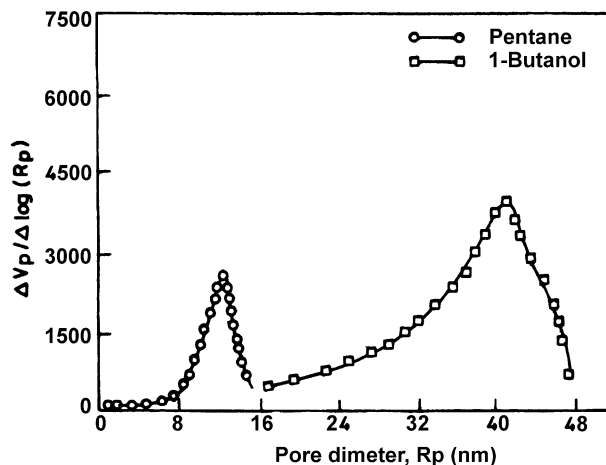


Fig. 3. Pore size distributions obtained by nitrogen adsorption/desorption of PVdF-HFP films prepared with (a) pentane and (b) 1-butanol as non-solvents.

by the phase inversion technique with pentane, as the non-solvent seems to be better than Celgard 2400 as far as pore diameters and surface area are concerned. The films prepared with 1-butanol appear to be very similar to Celgard separators.

These results demonstrate that the nanoscale morphology of the phase-separated membrane may be tailored by the nature of the non-solvent used. The smaller pore diameters of the films obtained with pentane may be attributed to (i) the linearity of the molecules and a corresponding smaller escape path for molecules during slow evaporation and (ii) the aliphatic, non-polar hydrocarbon nature of these molecules which lessens interaction with the hetero atoms in the PVdF-HFP co-polymer chain. On the other hand, the 1-butanol molecule is bulky, making it require an escape route that is larger in size.

Characterization of the nanoparticle cathode was also done. Fig. 4 shows the XRD patterns of $\text{LiCr}_{0.01}\text{Mn}_{1.99}\text{O}_4$ calcined at various temperatures in air. The crystallinity is increased with the increase of temperature, which is made evident by the sharpness of the peaks [20]. The impurity peaks observed at 22 and 53° in the XRD patterns are due to the formation of Mn_2O_3 during firing. The impurity peaks disappeared (indicated with an asterisk in the figure) for the samples heated at 800 °C. The presence of impurity peaks at lower temperatures may be due to the large amount of carbon content in the precursor, which tends to reduce the Mn ion during firing and favors the formation of Mn_2O_3 [21].

XRD peaks of $\text{LiCr}_{0.01}\text{Mn}_{1.99}\text{O}_4$ and the $\text{LiCr}_{0.01}\text{Mn}_{1.99}\text{O}_4$ ball milled for 2 h are shown in Fig.

5. After 2 h of ball milling we observe a decrease in intensity as well as broadening of the XRD peaks.

An AFM image (Fig. 6) reveals that the particle size of the spinel ranges from approximately 100 to 200 nm. These particles are agglomerated due to a high degree of crystallization at high temperature. It has been shown [16] that these nano crystalline grains and the strain, that develops at grain boundaries, give rise to XRD peak broadening. The formation of nano grains through ball milling may be due to two processes: (i) the particles are broken into nano particles, which may subsequently adhere back together and, (ii) during the ball milling process because of hard agglomerates, many nanograins could have been generated within larger crystals due to the action of defects.

The discharge capacities as a function of the cycle number of typical samples are shown in Fig. 7. The specific capacities for the cells made with $\text{LiCr}_{0.01}\text{Mn}_{1.99}\text{O}_4$ are 118 and 120 mA h g^{-1} , respectively, for the membranes prepared with pentane and 1-butanol. From our earlier studies [10], it has been reported that the conductivity values are higher for the films prepared with pentane than those prepared with 1-butanol. However, only this slight increase in specific capacity is observed for the membrane made using pentane. In contrast, the discharge capacity, as a function of cycle number for ball milled $\text{LiCr}_{0.01}\text{Mn}_{1.99}\text{O}_4$, is found to be significantly higher than the non-ball milled cathode. It has been suggested

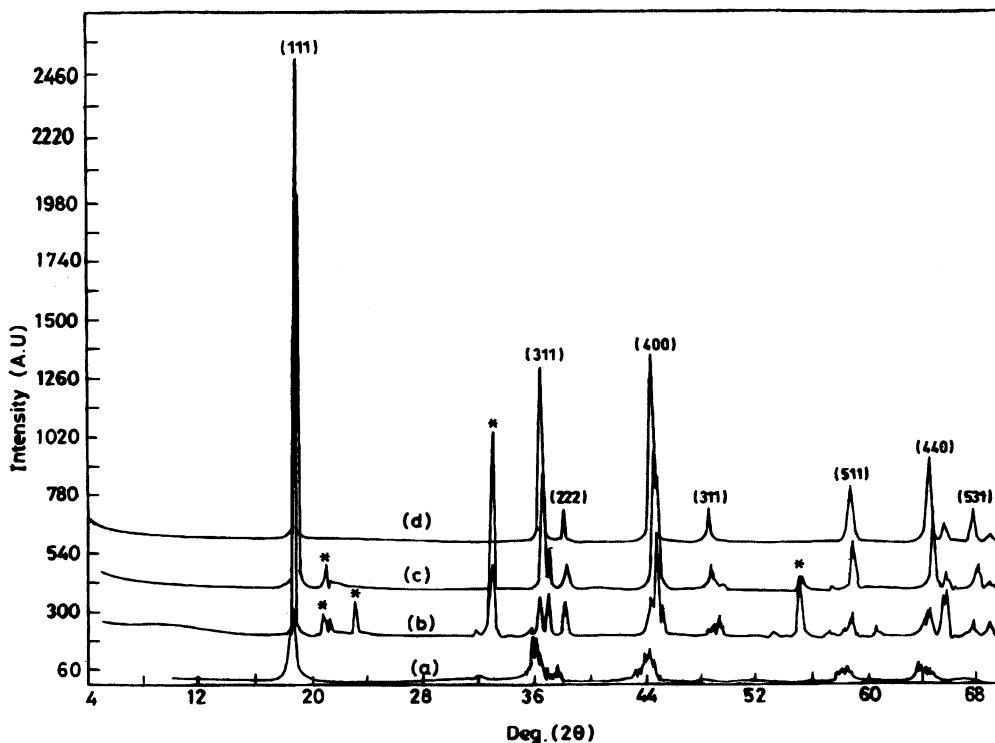


Fig. 4. Powder XRD patterns of $\text{LiCr}_{0.01}\text{Mn}_{1.99}\text{O}_4$; (a) as prepared and fired in air at (b) 400 °C, (c) 600 °C, and (d) 800 °C. The * corresponds to Mn_2O_3 .

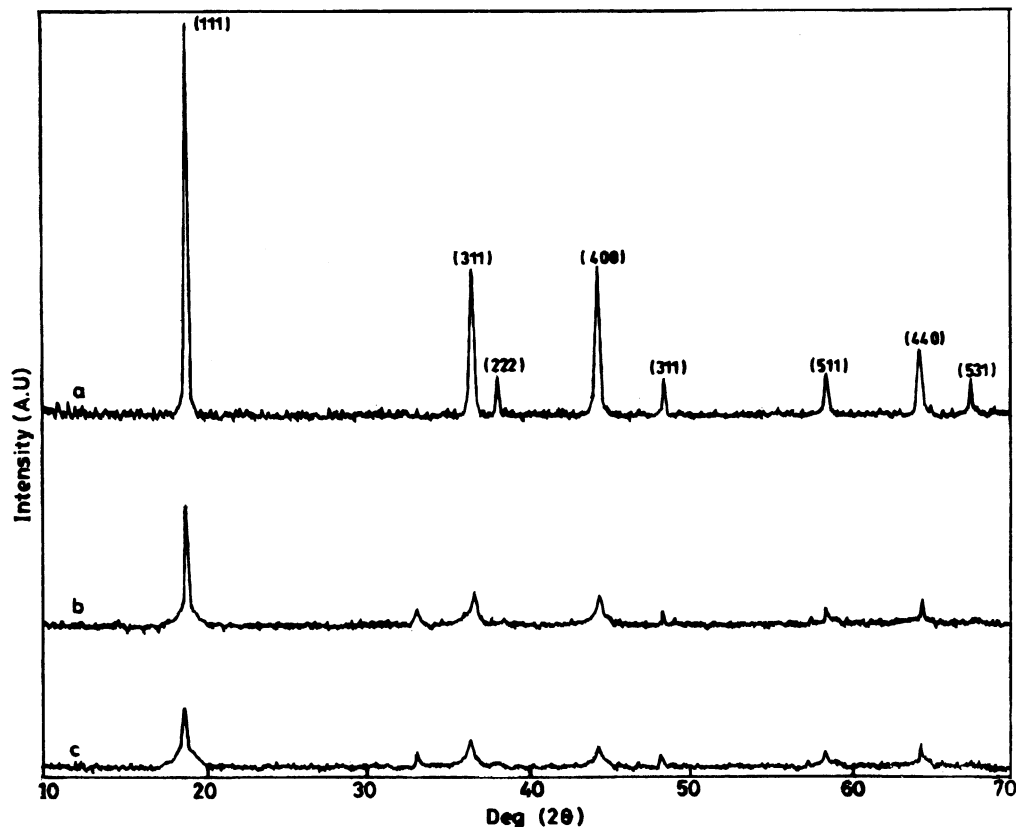


Fig. 5. XRD patterns of (a) $\text{LiCr}_{0.01}\text{Mn}_{1.99}\text{O}_4$, (b) $\text{LiCr}_{0.01}\text{Mn}_{1.99}\text{O}_4$ ball milled for an intermediate time, and (c) $\text{LiCr}_{0.01}\text{Mn}_{1.99}\text{O}_4$ ball milled for 2 h.

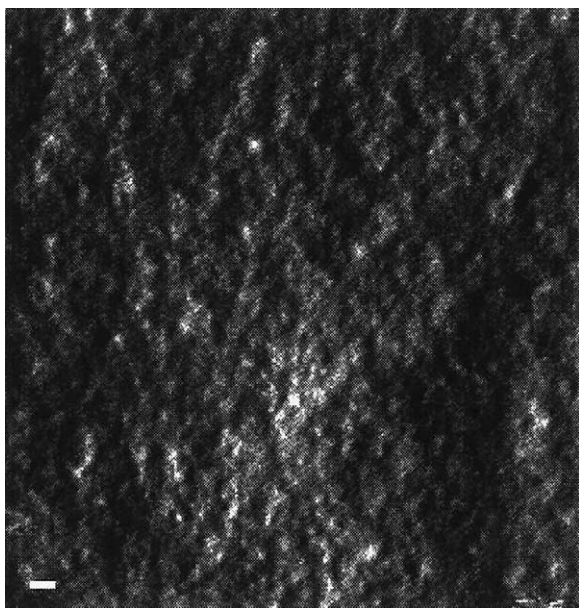


Fig. 6. AFM deflection image of $\text{LiCr}_{0.01}\text{Mn}_{1.99}\text{O}_4$ ball milled for 2 h. White bar in the lower left part of the image represents 200 nm.

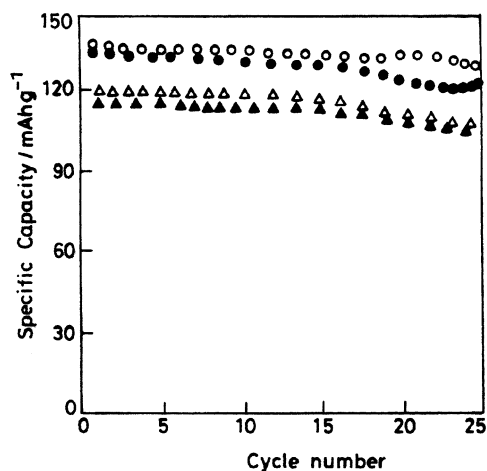


Fig. 7. Cycling performance of $\text{LiCr}_{0.01}\text{Mn}_{1.99}\text{O}_4$ cells employing PVdF-HFP membranes. Without cathode ball milling; with pentane as non-solvent (Δ), with 1-butanol as non-solvent (\blacktriangle). With cathode ball milling; with pentane as non-solvent (\circ), with 1-butanol as non-solvent (\bullet).

[16], that ball milling improves the cycle life of cathode materials for rechargeable lithium batteries and improves specific capacity due to the increase of lithium

ion conductivity resulting from smaller particle sizes. This work seems to support this finding. A slight decrease in the specific capacities with time is noted for all systems studied. The reason for this is unknown and will be investigated in future studies.

4. Conclusions

The PVdF-HFP co-polymer membranes prepared by phase inversion techniques with pentane as a non-solvent exhibited smaller pore sizes and a higher BET surface area than those prepared with 1-butanol. Although the physical properties such as porosity and pore morphology of the membranes vary with the nature of the non-solvent, only slight changes in the charge–discharge characteristics could be attributed to these changes in the polymer membrane. A simple ball milling process, which forms nanoparticles, is an effective way to increase the specific capacity of the cathode materials. The doped nano crystalline cathode material is found to be suitable for charge–discharge applications when highly nanoporous membranes are used as separators in secondary lithium batteries.

Acknowledgements

The authors would like to thank the Office of Naval Research through grant N00014-01-1-0724 for funding this work.

References

- [1] S. Paneri, B. Scrosati, *J. Power Sources* 90 (2000) 13.
- [2] W.H. Meyer, *Adv. Mater.* 10 (1998) 439.
- [3] A. Manuel Stephan, N.G. Renganathan, S. Pitchumani, N. Muniyandi, *J. Power Sources* 8182 (1999) 752.
- [4] A. Manuel Stephan, N.G. Renganathan, S. Pitchumani, N. Muniyandi, *J. Power Sources* 83 (2000) 80.
- [5] A. Manuel Stephan, N.G. Renganathan, S. Pitchumani, N. Muniyandi, *Solid State Ionics* 132 (2001) 123.
- [6] A.S. Gozdz, C.W. Schmutz, J.M. Tarascon, P.C. Warren, US Patent 5,540 741, 1997.
- [7] J.M. Tarascon, A.S. Gozdz, C. Schmutz, C.W. Schmutz, P.C. Warren, *Solid State Ionics* 86–88 (1997) 741.
- [8] J.Y. Song, Y.Y. Wang, C.C. Wan, *J. Power Sources* 77 (2000) 183.
- [9] H. Wang, H. Huang, S.L. Wunder, *J. Electrochem. Soc.* 147 (2000) 2853.
- [10] Y. Saito, H. Kataoka, A. Manuel Stephan, *Macromolecules* 34 (2001) 6455.
- [11] A. Manuel Stephan, H. Kataoka, Y. Saito, *Solid State Ionics*, 2002, in press.
- [12] A. Manuel Stephan, Y. Saito, *Solid State Ionics* 148 (2002) 475.
- [13] Y. Gao, J.R. Dahn, *Solid State Ionics* 69 (1994) 59.
- [14] V. Manev, W. Ebner, W. Thompson, S. Dow, US Patent 5, 961,949, 1999.
- [15] C.S. Wang, G.T. Wu, W.Z. Li, *J. Power Sources* 76 (1998) 1.
- [16] S.H. Kang, J.B. Goodenough, L.K. Rabenberg, *Electrochem. Solid State Lett.* 4 (5) (2001) A49–A51.
- [17] A. Manuel Stephan, D. Teeters, *Electrochim. Acta*, in press.
- [18] A. Manuel Stephan, D. Teeters, *Solid State Electrochem.*, submitted for publication.
- [19] J.Y. Song, Y.Y. Wang, C.C. Wan, *J. Electrochem. Soc.* 147 (2000) 3219.
- [20] J. Kim, A. Manthiram, *Electrochem. Solid State Lett.* 4 (5) (2001) A49–A51.
- [21] S. Choi, A. Manthiram, *J. Electrochem. Soc.* 147 (2000) 1623.